

1 This is the final, post-review version of the following published paper:

2 FRANKLIN, D.J., AIRS, R.L., FERNANDES, M., BELL, T.G., BONGAERTS, R.J., BERGES, J.A. & MALIN, G. 2012.  
3 Identification of senescence and death in *Emiliana huxleyi* and *Thalassiosira pseudonana*: Cell staining,  
4 chlorophyll alterations, and dimethylsulfoniopropionate (DMSP) metabolism. *Limnology & Oceanography*  
5 57(1): 305-317. DOI: 10.4319/lo.2012.57.1.0305.

6

7 Identification of senescence and death in *Emiliana huxleyi* and *Thalassiosira pseudonana*:

8 Cell staining, chlorophyll alterations, and dimethylsulphonioopropionate (DMSP) metabolism

9

10 Daniel J. Franklin,<sup>a,b,\*</sup> Ruth L. Airs,<sup>c</sup> Michelle Fernandes,<sup>b</sup> Thomas G. Bell,<sup>b</sup> Roy J.

11 Bongaerts,<sup>d</sup> John A. Berges,<sup>e</sup> Gill Malin<sup>b</sup>

12

13 <sup>a</sup> School of Applied Sciences, Bournemouth University, Talbot Campus, Fern Barrow, Poole,

14 United Kingdom

15 <sup>b</sup> Laboratory for Global Marine and Atmospheric Chemistry, School of Environmental

16 Sciences, University of East Anglia, Norwich, United Kingdom

17 <sup>c</sup> Plymouth Marine Laboratory, Prospect Place, Plymouth, United Kingdom

18 <sup>d</sup> Institute of Food Research, Norwich Research Park, Norwich, United Kingdom

19 <sup>e</sup> Department of Biological Sciences, University of Wisconsin-Milwaukee, Milwaukee,

20 Wisconsin

21

22 \* Corresponding author: [dfranklin@bmath.ac.uk](mailto:dfranklin@bmath.ac.uk)

23 **Acknowledgements**

24           We thank the U.K. Natural Environment Research Council for funding this research  
25 (NE/E003974/1) and Rob Utting and Gareth Lee for technical help. We also thank the two  
26 anonymous reviewers who provided constructive comments. Additional support was provided  
27 by a British Council studentship to M.F. (UK India Education and Research Initiative).

## 28 **Abstract**

29           We measured membrane permeability, hydrolytic enzyme, and caspase-like activities  
30 using fluorescent cell stains to document changes caused by nutrient exhaustion in the  
31 coccolithophore *Emiliania huxleyi* and the diatom *Thalassiosira pseudonana*, during batch-  
32 culture nutrient limitation. We related these changes to cell death, pigment alteration, and  
33 concentrations of dimethylsulphide (DMS) and dimethylsulfoniopropionate (DMSP) to assess  
34 the transformation of these compounds as cell physiological condition changes. *E. huxleyi*  
35 persisted for 1 month in stationary phase; in contrast, *T. pseudonana* cells rapidly declined  
36 within 10 days of nutrient depletion. *T. pseudonana* progressively lost membrane integrity  
37 and the ability to metabolise 5-chloromethylfluorescein diacetate (CMFDA; hydrolytic  
38 activity) whereas *E. huxleyi* developed two distinct CMFDA populations and retained  
39 membrane integrity (SYTOX green). Caspase-like activity appeared higher in *E. huxleyi* than  
40 *T. pseudonana* during the post-growth phase, despite a lack of apparent mortality and cell  
41 lysis. Photosynthetic pigment degradation and transformation occurred in both species after  
42 growth; chlorophyll *a* (Chl *a*) degradation was characterised by an increase in the ratio of  
43 methoxy Chl *a*:Chl *a* in *T. pseudonana* but not in *E. huxleyi*, and the increase in this ratio  
44 preceded loss of membrane integrity. Total DMSP declined in *T. pseudonana* during cell  
45 death and DMS increased. In contrast, and in the absence of cell death, total DMSP and DMS  
46 increased in *E. huxleyi*. Our data show a novel chlorophyll alteration product associated with  
47 *T. pseudonana* death, suggesting a promising approach to discriminate non-viable cells in  
48 nature.

## 49 **Introduction**

50           Phytoplankton cell physiology is fundamental to global biogeochemical cycles  
51 because the mediation of biogeochemical processes by phytoplankton, such as the production  
52 of the trace gas dimethylsulphide and carbon fixation, strongly depends on cell physiological  
53 state. Non-dividing alternative physiological states include senescence, quiescence  
54 (dormancy) and death (Franklin et al. 2006). Such alternative states are poorly understood,  
55 especially in eukaryotic marine phytoplankton, but are likely to be significant in natural  
56 assemblages. Some progress has been made in recognising cell state in the laboratory: the  
57 morphological changes associated with nutrient limitation in batch cultures have been studied,  
58 and similarities with metazoan programmed cell death (PCD; Bidle and Falkowski 2004;  
59 Franklin et al. 2006) have been described in certain phytoplankton (e.g., *Dunaliella*  
60 *tertiolecta*; Segovia and Berges 2009). An improved ability to recognise senescent, quiescent,  
61 moribund and dead cells within microbial populations is important because a substantial  
62 fraction of natural phytoplankton biomass may be non-viable (Veldhuis et al. 2001; Agusti  
63 2004) and yet viability will be a major driver of primary production and biogeochemistry.  
64 Accurate estimation of phytoplankton primary production through remote sensing could be  
65 improved by practical recognition of different physiological states. Although efforts to  
66 understand physiological change in terms of variable pigment content within  
67 photosynthesizing cells via remote sensing (Behrenfeld and Boss 2006) offers a useful way to  
68 assess natural physiological variability, the ability to discriminate ‘viability’ cannot currently  
69 be achieved by remote sensing. In order to achieve this, we need to find robust indicators of  
70 cell death that have value in the field. As part of this effort we undertook a laboratory study  
71 which aimed to provide tools for field assessments of phytoplankton viability.

72 Chlorophyll *a* (Chl *a*) alteration during senescence is of great interest in organic  
73 geochemistry (Louda et al. 2002; Szymczak-Zyla et al. 2008) and may be useful as a field  
74 signal of phytoplankton cell death. One potential difficulty is that observations of Chl *a*  
75 alteration have not been explicitly linked with microalgal growth phase or physiological state  
76 (Louda et al. 2002) limiting its usefulness as an indicator of cell death. In general, increased  
77 concentrations of chlorophyll oxidation products have been observed in nutrient-depleted  
78 cells, but it is likely that specific chlorophyll transformation pathways vary between species  
79 (Bale 2010). Initial investigations into pigment alteration and cell viability in natural  
80 phytoplankton assemblages (using SYTOX green staining) have used pigment fluorescence to  
81 assess chlorophyll loss (Veldhuis et al. 2001). Such approaches have been useful, but miss  
82 vital information on the early alteration of chlorophyll. Early alteration mostly gives  
83 structures with indistinguishable absorption and fluorescence properties from the parent  
84 compound and which are, therefore, invisible to fluorescence-based methods. Molecular  
85 structures resulting from early stage alterations can be produced by the reaction of chlorophyll  
86 *a* with, for example, the reactive oxygen species H<sub>2</sub>O<sub>2</sub> (Walker et al. 2002), and likely occur  
87 in conjunction with cell death because reactive oxygen species are associated with cell death.  
88 High-performance liquid chromatography (HPLC) methods vary in their ability to separate  
89 and detect chlorophyll allomers (Airs et al. 2001) and a suitable method has not yet been  
90 applied to the model species of this study in combination with independent measures of cell  
91 viability. In our study we link an assessment of viability (using flow cytometry) with a high  
92 resolution HPLC method (Airs et al. 2001), in combination with liquid chromatography-mass  
93 spectrometry (LC-MS) characterisation, in order to assess the pigment changes associated  
94 with changing physiological state.

95           Dimethyl sulphide (DMS) is the main natural source of reduced sulphur to the  
96 troposphere (Simó 2001). DMS is a volatile trace gas which promotes aerosol formation and  
97 thereby affects global climate (Charlson et al. 1987). The molecular precursor of DMS, the  
98 compatible solute dimethylsulphoniopropionate (DMSP), occurs at high intracellular  
99 concentrations (100–400 mmol L<sup>-1</sup>) in coccolithophores such as *E. huxleyi* (Keller et al.  
100 1989), and at lower concentrations in diatoms (Keller and Korjeff-Bellows 1996). DMSP can  
101 be released to the seawater dissolved organic carbon pool through grazing, viral lysis, cell  
102 senescence or active exudation, but information on the latter two processes is very limited  
103 (Stefels et al. 2007). Intracellular DMSP concentration increases in some phytoplankton  
104 species when growth is limited due to CO<sub>2</sub> or Fe limitation, Ultraviolet light exposure, toxic  
105 levels of cupric ions or addition of hydrogen peroxide (Sunda et al. 2002). On this basis  
106 Sunda et al. (2002) suggested that DMSP and its lysis products DMS and acrylate may form  
107 an antioxidant cascade. This would presumably increase the survival of phytoplankton cells  
108 during conditions associated with oxidative stress and elevated levels of reactive oxygen  
109 species. An alternative hypothesis is that under conditions of unbalanced growth an overflow  
110 mechanism operates whereby excess energy and reduced compounds are used for DMSP  
111 production to ensure the continuation of other metabolic pathways (Stefels 2000). Several  
112 studies have shown that nitrogen limitation leads to increased DMSP concentration (Stefels et  
113 al. 2007). For example, Harada et al. (2009) recently found that intracellular DMSP  
114 concentration increased from 2.1 to 15 mmol L<sup>-1</sup> in 60 h when the diatom *Thalassiosira*  
115 *oceanica* was grown in low nitrate medium, and this was especially notable when the cells  
116 reached the stationary phase. In addition, Archer et al. (2010) showed that under conditions of  
117 acute photo-oxidative stress *Emiliania huxleyi* rapidly accumulated DMSP to a level that was  
118 21% above that of control cells. Such processes must require an intact and functioning

119 metabolism, and a logical next step is to assess DMSP and DMS production in parallel with  
120 assessments of pigments and cell viability.

121 *Emiliana huxleyi* and *Thalassiosira pseudonana* are good model species for the major  
122 calcifying and silicifying phytoplankton groups and are therefore highly relevant for an  
123 investigation into cell physiology and its relationship with biogeochemical processes. We  
124 grew cells through the batch cycle and used flow cytometry to examine changes in  
125 physiological state using fluorescent cell stains for membrane permeability and enzyme  
126 activity. In conjunction with these cell viability assays we investigated the time course of  
127 pigment alteration using a high resolution HPLC-LC-MS method that allows the separation  
128 and detection of chlorophyll allomers (Airs et al. 2001). In addition, we analysed for DMSP  
129 and DMS to address the knowledge gap on the production of these compounds relative to cell  
130 viability.

## 131 **Methods**

132 *Cell culture and growth measurements* Unialgal duplicate cultures of *Emiliana*  
133 *huxleyi* (CCMP 1516; calcifying) and *Thalassiosira pseudonana* (CCMP 1335) were grown  
134 in 500 mL of ESAW/5 media (Enriched Seawater, Artificial Water; Harrison et al. 1980) in  
135 1000 mL borosilicate conical flasks. Silica was omitted in *E. huxleyi* media.  
136 Photosynthetically active radiation was supplied at  $100 \mu\text{mol photons m}^{-2} \text{ s}^{-1}$  (Biospherical  
137 Instruments QSL 2101) from cool white fluorescent tubes, on a 14 h:10 h light:dark cycle  
138 (08:00 h – 22:00 h) at a constant temperature of 17°C. Each day at the same time (10:00 h)  
139 biomass was quantified as cell number, cell (or coccosphere in the case of *Emiliana huxleyi*)  
140 volume (Beckman Coulter MS3), and fluorescence (Heinz-Walz GmbH; PHYTO-PAM  
141 equipped with a PHYTO-ED measuring head). The efficiency of Photosystem II ( $F_V:F_M$ ; 30  
142 minute dark-acclimation) was measured at the same time.

143 *Flow cytometry and cell staining* Fluorescent staining analyses were conducted with  
144 three molecular probes. Two of these have been described as ‘live/dead’ stains; SYTOX green  
145 can be used to measure changes in membrane permeability (Veldhuis et al. 1997; ‘dead’ cells)  
146 and CMFDA is cleaved by a variety of enzymes indicating hydrolytic enzymatic activity (D.J.  
147 Franklin and J.A. Berges unpubl. data; Garvey et al. 2007; ‘live’ cells). SYTOX green  
148 (Invitrogen S7020) was applied at a final concentration of  $0.5 \mu\text{mol L}^{-1}$  during a 10 minute,  
149 culture temperature, dark incubation. Uptake of the stain was compared with unstained  
150 controls via flow cytometry (BD FACScalibur). SYTOX green was diluted from the supplied  
151  $5 \text{ mmol L}^{-1}$  in dimethyl sulphoxide stock solution to  $0.1 \text{ mmol L}^{-1}$  in Milli-Q water and stored  
152 frozen ( $-20^{\circ}\text{C}$ ) prior to use. CMFDA (5-chloromethylfluorescein diacetate; Invitrogen C2925)  
153 was added to a final concentration of  $10 \mu\text{mol L}^{-1}$  and incubated for 60 min at culture  
154 temperature and light conditions. CMFDA was diluted to a concentration of  $1 \text{ mmol L}^{-1}$  in  
155 acetone prior to use (Peperzak and Brussaard 2011) before aliquoting and storage at  $-20^{\circ}\text{C}$ .  
156 SYTOX-green and CMFDA final concentration and incubation time were optimised prior to  
157 use using heat-killed cells ( $80^{\circ}\text{C}$ , 5 min) and the ‘maximum fluorescence ratio’ approach  
158 (Brussaard et al. 2001). We used an adaptation of the protocol of Bidle and Bender (2008) to  
159 detect caspase-like activity: cells were stained in vivo with a fluorescein isothiocyanate  
160 (FITC) conjugate of carbobenzoxy-valyl-alanyl-aspartyl-[O-methyl]-fluoromethylketone to  
161 label cells containing activated caspases (CaspACE; Promega G7462). Caspases are proteases  
162 thought to be specific to programmed cell death (*see* Discussion). CaspACE was added to  
163 cells at a final concentration of  $0.5 \mu\text{mol L}^{-1}$  and incubated for 30 min at culture temperature  
164 in the dark, before flow cytometric analysis. For all stains working stocks were kept at  $-20^{\circ}\text{C}$   
165 before use. We used Milli-Q water as a sheath fluid, analyses were triggered on red  
166 fluorescence, using ‘lo’ flow (approximately  $20 \mu\text{L min}^{-1}$ ), and 10,000 events were collected.  
167 We used an event rate between 100 and 400 cells  $\text{s}^{-1}$  to avoid coincidence and when needed,



168 samples were diluted in 0.1  $\mu\text{m}$ -filtered artificial seawater prior to analysis. Flowset beads  
169 (Beckman-Coulter) were analysed at the beginning of each set of measurements and bead  
170 fluorescence was used to normalize stain fluorescence (Marie et al. 2005).

171

172         *Photosynthetic pigments* Culture samples (20-25 mL) were centrifuged (5300 x g, 20  
173 min, 8°C), the supernatant discarded and cells were flash frozen in liquid N<sub>2</sub> and stored at -  
174 80°C until analysis. Samples were extracted in 0.5 mL acetone under dim light by sonication  
175 (Amplitude 35%; Vibra Cell Probe; Sonics) for 45 s. The extract was clarified by  
176 centrifugation (10,956 x g, Microcentrifuge 5415; Eppendorf). Reversed-phase high  
177 performance liquid chromatography (HPLC) was conducted using an Agilent 1200 system  
178 with photodiode array detector. Instrument control, data processing and analysis were  
179 performed using Chemstation software. Separations were performed in the reversed-phase  
180 mode using two Waters (Milford, MA, USA) Spherisorb ODS2 C18 3  $\mu\text{m}$  columns (150 x 4.6  
181 mm i.d.) in-line with a pre-column containing the same phase (10 x 5 mm i.d.). A  
182 Phenomenex pre-column filter (Security Guard, ODS C18, 4 x 3 mm i.d.) was used to prevent  
183 rapid deterioration of the pre-column. Elution was carried out using a mobile phase gradient  
184 comprising acetonitrile, methanol, 0.01 mol L<sup>-1</sup> ammonium acetate and ethyl acetate at a flow  
185 rate of 0.7 mL min<sup>-1</sup> (Method C in Airs et al. 2001). All solvents were HPLC grade. Liquid  
186 chromatography-mass spectrometry (LCMS) analysis was performed using an Agilent 1200  
187 HPLC with photodiode array detection coupled via an atmospheric pressure chemical  
188 ionisation (APCI) source to an Agilent 6330 ion trap mass spectrometer. The HPLC  
189 conditions used were as described above. The MS was operated in the positive ion mode.  
190 LCMS settings were as follows: drying temperature 350°C, APCI vaporiser temperature  
191 450°C, nebulizer 413700 Pa, drying gas 5 L min<sup>-1</sup>, capillary voltage -4500 V. Methanoic acid  
192 was added to the HPLC eluent post column at a flow rate of 5  $\mu\text{L min}^{-1}$  to aid ionisation (Airs

193 and Keely 2000). Using a combination of high resolution HPLC and LCMS (Airs et al. 2001)  
194 enabled separation and structural assignment of chlorophyll alteration products present in the  
195 samples, as well as routinely detected chlorophylls and carotenoids.

196 *DMSP and DMS* Five mL of culture was sampled using gas-tight syringes and gently  
197 filtered (25 mm Whatman GF/F) using a Swinnex unit. The filter was then placed into a 4 mL  
198 vial containing 3 mL of 0.5 mol NaOH and immediately closed with a screw cap containing a  
199 PTFE/silicone septum (Alltech). The vials were kept in the dark and placed in a constant  
200 temperature heating block at 30°C overnight to equilibrate. The headspace of the vial was  
201 then analysed for DMS by piercing the septum with a gas-tight syringe and injecting 50  $\mu\text{L}$   
202 into a gas chromatograph (Shimadzu GC-2010 with flame photometric detection). The  
203 amount of DMSP particulate on the filter was then calculated with reference to standard  
204 curves and expressed as a concentration in the cells (Steinke et al. 2000). The filtrate was  
205 purged immediately to analyse culture DMS concentration. The filtrate was purged for 15 min  
206 ( $\text{N}_2$ , 60 mL  $\text{min}^{-1}$ ) in a cryogenic purge-and-trap system; DMS was trapped in a Teflon loop  
207 ( $-150^\circ\text{C}$ ), flash evaporated by immersing the loop in boiling water and then injected into the  
208 GC (Turner et al. 1990). After purging the DMS from the filtrate, the concentration of  
209  $\text{DMSP}_{\text{dissolved}}$  was determined by transferring 4 mL of the purged filtrate into a 20 mL crimp  
210 vial, to which 1 mL of 10 mol NaOH was added and topped up with 10 mL distilled water to  
211 maintain a constant analytical volume of 15 mL. The vial was immediately closed with a  
212 Teflon coated septum and later analysed by the headspace technique.  $\text{DMSP}_{\text{total}}$  was measured  
213 in an unfiltered volume of culture hydrolysed with 0.5 mL of 10 mol NaOH in a vial sealed  
214 gas-tight with a PTFE-silicone septum.

## 215 **Results**

### 216 *Cell culture and growth measurements*

217 To minimise the presence of dead cells and debris in the cultures at the beginning of  
218 the experiment, cultures were closely monitored and grown in semi-continuous mode before  
219 measurements commenced. From preliminary work it was clear that both *Emiliania huxleyi*  
220 and *Thalassiosira pseudonana* biomass would consistently achieve a final yield of  
221 approximately  $2.5 \times 10^6$  cells mL<sup>-1</sup> with a specific growth rate ( $\mu$  d<sup>-1</sup>) of 0.6 under our culture  
222 conditions. By calculation, nitrogen should have been limiting in both species at this point  
223 assuming cells were using nutrients in the Redfield ratio. We performed ‘add-back’  
224 experiments to test what controlled limitation (data not shown). These experiments indicated  
225 that for *T. pseudonana* nitrogen clearly caused growth limitation; when nitrate was added  
226 back cell number increased. The pattern for *E. huxleyi* was less clear as no obvious increase in  
227 *E. huxleyi* biomass was stimulated by adding back either nitrate or phosphate. After the onset  
228 of stationary phase *E. huxleyi* cell number remained constant for 20 days whereas *T.*  
229 *pseudonana* cell number began to decline after 5 days, and over the next 20 days declined by  
230 65% (Fig. 1A). *E. huxleyi* coccosphere volume increased after the growth phase from a mean  
231 of about 35  $\mu\text{m}^3$  to almost 80  $\mu\text{m}^3$  at the end of the stationary phase. *T. pseudonana* also  
232 increased in cell volume, but by less than *E. huxleyi* coccosphere volume; the increase in cell  
233 volume stabilised after the growth phase at about 50  $\mu\text{m}^3$  (Fig. 1A). *T. pseudonana* dark-  
234 acclimated  $F_V:F_M$  (Maximum photosystem II efficiency; PS II efficiency; Kromkamp and  
235 Forster 2003) declined from a maximum of 0.6 in early log-phase to zero after 5 days in  
236 stationary phase. *E. huxleyi* dark-acclimated  $F_V:F_M$  remained constant at approximately 0.5  
237 (Fig. 1B). Culture fluorescence declined after the onset of stationary phase in both species  
238 (Fig. 1C). During this decline it was possible to discriminate two subpopulations by flow  
239 cytometry (*see below*).

240

241 *Flow cytometry and cell staining*

242 Light scattering. Over the transition from growth to stationary phase *Emiliania huxleyi*  
243 forward scatter increased and side scatter became more variable. An increase in *T.*  
244 *pseudonana* forward scatter was also evident over the transition but no obvious change in side  
245 scatter developed (data not shown).

246 Pigment fluorescence. During growth all *Emiliania huxleyi* cells had the same, slightly  
247 increasing, pigment fluorescence (data not shown). During the stationary phase all cells  
248 declined in pigment fluorescence and a 'low-red' subpopulation developed (Fig. 2). This  
249 subpopulation doubled in size during the stationary phase, from approximately 6 to 12% of all  
250 cells. Low-red *E. huxleyi* cells were not obviously different in terms of forward and side  
251 scatter compared to 'normal' cells. *T. pseudonana* cells also declined in average pigment  
252 fluorescence after the onset of stationary phase and low-red cells accounted for almost 50% of  
253 cells towards the end of the sampling period. As in *E. huxleyi*, *T. pseudonana* low-red cells  
254 did not obviously differ from normal cells in their forward and side scatter characteristics  
255 (data not shown).

256 SYTOX green staining. *E. huxleyi* showed <5% labeled cells throughout the  
257 experiment; neither the low-red nor normal cells labeled with SYTOX green, indicating that  
258 almost all cells, of both cell types, had intact plasma membranes over the duration of the  
259 monitoring period. In contrast, *T. pseudonana* had low numbers of labeled cells (<2%) until  
260 the stationary phase whereupon the percentage of labeled cells rose rapidly to a maximum of  
261 25% on the last sampling day (Fig. 3).

262 CMFDA staining. Within the growth phase *E. huxleyi* cells showed clear differences  
263 in CMFDA metabolism. Most cells metabolised the probe and become highly fluorescent;  
264 however about 20% of cells showed no increased fluorescence and were similar to unstained  
265 controls (Fig. 4A). This difference remained roughly constant throughout the stationary phase  
266 (Fig. 4B). Further, in *E. huxleyi* the 'high CMF' population increased their CMFDA

267 metabolism in the stationary phase (Fig. 4C). The low red *E. huxleyi* cells that increased  
268 slightly in abundance throughout the experiment did not metabolise the probe; low red cell  
269 green fluorescence was comparable to unstained cells. *T. pseudonana* did not show this intra-  
270 population variability; all cells within the population exhibited a significant decline (linear  
271 regression;  $p=0.001$ ) in CMFDA fluorescence over the transition from active growth to  
272 stationary phase (Fig. 4C). However, even in the death phase, *T. pseudonana* cells showed  
273 CMFDA fluorescence that was elevated relative to unstained controls (data not shown).

274       CaspACE staining. *E. huxleyi* CaspACE fluorescence increased during the experiment  
275 with both types of cells (normal and low red) showing a similar level of fluorescence due to  
276 CaspACE binding. Amongst normal *E. huxleyi* cells there was a significant increase (linear  
277 regression;  $p=0.001$ ) in CaspACE binding over time (Fig. 5). There was no significant trend  
278 (linear regression;  $p=0.05$ ; Fig. 5) in *T. pseudonana* CaspACE fluorescence with time, and as  
279 with *E. huxleyi* cells, there was no obvious difference between normal and low-red *T.*  
280 *pseudonana* cells (data not shown).

#### 281 *Photosynthetic pigments*

282       Chemical assignment. During reversed-phase HPLC, chlorophyll allomers typically  
283 elute in the region of the chromatogram immediately prior to chlorophyll *a* (Walker et al.  
284 2002) and most exhibit UV-vis spectra indistinguishable from chlorophyll *a*. In extracts from  
285 this study, five components (I-V, Fig. 6) eluted in the region expected for chlorophyll  
286 allomers. Components I and III were assigned as  $13^2$ -hydroxy-chlorophyll *a* (*see* structure  
287 inset, Fig. 6) and  $13^2$ -hydroxy-chlorophyll *a'*, and components IV and V were assigned as (*S*)-  
288  $13^2$ -methoxy-chlorophyll *a* and (*R*)- $13^2$ -methoxy-chlorophyll *a*, respectively, by comparison  
289 to published MS/MS data (Table 1; Walker et al. 2002). Component II exhibited similar  
290 analytical data to Chl *a* (Table 1), showing a 2 Da difference in protonated molecule and  
291 common major ions in MS<sup>2</sup> (Table 1). The phytol chain of chlorophyll *a* is lost as phytadiene,

292 resulting in a loss of 278 Da during APCI-LCMS<sup>n</sup> (Airs et al. 2001; Table 1). The loss of 276  
293 Da from the protonated molecule of component II indicates that the structural difference from  
294 Chl *a* originates on the phytol chain and is likely to be due to an additional double bond. This  
295 component has been assigned previously in a culture of *Pavlova gyrans* (Bale 2010). One of  
296 the final stages in the biosynthesis of chlorophyll *a* is the conversion of geranylgeraniol to  
297 phytol by saturation of three of its double bonds (Rudiger 2006). Component II, referred to  
298 from here on as Chl *a*<sub>P276</sub>, may therefore be a biosynthetic precursor to chlorophyll *a*.

### 299 *Pigment changes during growth limitation*

300 Of the alteration products observed, methoxychlorophyll *a* was present at highest  
301 concentrations relative to chlorophyll *a* in both *Emiliania huxleyi* and *Thalassiosira*  
302 *pseudonana* (Fig. 7A). In both cultures Chl *a*<sub>P276</sub> was highest in the active growth phase,  
303 consistent with its assignment as a biosynthetic precursor to chlorophyll *a*. In *T. pseudonana*,  
304 methoxychlorophyll *a* increased relative to chlorophyll *a* during the transition from cell  
305 division to the stationary phase (Fig. 7A). The concentration of methoxychlorophyll *a* stayed  
306 high relative to chlorophyll *a* into the diatom death phase, before declining to undetectable  
307 levels (Fig. 7A). The ratio of hydroxychlorophyll *a*:Chl *a* showed a slight increase in *T.*  
308 *pseudonana* during the transition, mirroring the profile of methoxychlorophyll *a*. No increase  
309 in the ratio of methoxychlorophyll or hydroxychlorophyll *a* to chlorophyll *a* was observed in  
310 *E. huxleyi* cultures (Fig. 7A). The carotenoid:chlorophyll *a* ratio remained constant in *E.*  
311 *huxleyi* (Fig. 7B) but steadily increased in *T. pseudonana*. In *E. huxleyi*, the reduction in  
312 carotenoids closely tracked the reduction in chlorophyll, consistent with a controlled  
313 reduction of cellular pigment concentration. In *T. pseudonana*, the increase in the  
314 carotenoid:chlorophyll ratio occurred because of a more rapid decrease in chlorophyll relative  
315 to carotenoids.

### 316 *DMSP and DMS*

317 Over the course of the experiment, *E. huxleyi* cultures significantly (linear regression;  
318  $p=0.001$ ) accumulated DMSP ( $\text{DMSP}_{\text{total}}$ ) whereas *T. pseudonana*  $\text{DMSP}_{\text{total}}$  showed no  
319 significant relationship with time ( $p=0.05$ ). Within the *T. pseudonana* dataset however, a  
320 decline in  $\text{DMSP}_{\text{total}}$  is suggested within the stationary/death phase (Fig. 8A). The intracellular  
321 concentration of DMSP ( $\text{DMSP}_{\text{cell}}$ ; Fig. 8B) showed no significant trend with time ( $p=0.05$ ) in  
322 both species over the whole course of the experiment, and was consistent within the  
323 stationary/death phase at approximately  $120 \text{ mmol L}^{-1}$  (*E. huxleyi*) and  $35 \text{ mmol L}^{-1}$  (*T.*  
324 *pseudonana*). However, between days 0 and 10 there was a notable increase in *T. pseudonana*  
325  $\text{DMSP}_{\text{cell}}$  from  $0.7$  to  $34 \text{ mmol L}^{-1}$ . The divergence between  $\text{DMSP}_{\text{total}}$  and  $\text{DMSP}_{\text{cell}}$  in *E.*  
326 *huxleyi* can be explained by the increased coccosphere volume in stationary phase; *E. huxleyi*  
327 coccosphere volume increased with time (Fig. 1A). The concentration of DMS in both  
328 cultures increased significantly over the course of the experiment ( $p=0.05$ ). In *T. pseudonana*  
329 DMS increased from  $5 \text{ nmol L}^{-1}$  to  $90 \text{ nmol L}^{-1}$  and from  $10 \text{ nmol L}^{-1}$  to  $42 \text{ nmol L}^{-1}$  in *E.*  
330 *huxleyi* (Fig. 8C).  $\text{DMSP}_{\text{dissolved}}$  increased in both species after the growth phase, to around  $2$   
331  $\mu\text{mol L}^{-1}$  in *E. huxleyi* and around  $1.25 \mu\text{mol L}^{-1}$  in *T. pseudonana* (data not shown).

## 332 Discussion

333 The main finding of our work was that the response of the two model species to  
334 nutrient limitation was quite different. Establishing the specific nutrient that is limiting is  
335 important to place the work into an environmental context. Add-back experiments are a useful  
336 way of verifying the limiting nutrient (La Roche et al. 1993) and clearly indicated N-  
337 limitation as the cause of growth limitation in our *Thalassiosira pseudonana* cultures. The  
338 add-back data were ambiguous for *Emiliania huxleyi*. We suggest that the timing of the add-  
339 back is important and we may have been too late in adding the nutrients (which we did just  
340 before the plateau). We hypothesize that *E. huxleyi* cells may have already committed to

341 transforming into a ‘persister’ form by the time the extra nutrients were delivered and thus the  
342 add-back of limiting nutrient had no effect. We find the fact that Loebel et al. (2010) find  
343 similar patterns in *E. huxleyi* PS II efficiency, and biomass, under N-deprivation quite  
344 compelling as it provides support for N being the cause of growth limitation in our  
345 experiments. However, Loebel et al. (2010) used a different type of experimental manipulation  
346 (centrifugation of cells and resuspension in N-free media) which would have resulted in  
347 somewhat different environmental conditions for the cells. Regardless of the method of  
348 inducing N-limitation however, the tolerance of *E. huxleyi* to endure growth-limiting  
349 conditions were clearly superior to that of *T. pseudonana*.

350         Knowing whether cells are viable is important in order to scale metabolic parameters  
351 such as exudation rates or primary production (Garvey et al. 2007). In this study, we have  
352 linked an assessment of viability with the alteration of two classes of compounds important in  
353 biogeochemical cycles. Viability is ‘the quality or state of being viable; the capacity for  
354 living; the ability to live under certain conditions’ (Oxford English Dictionary), and in cell  
355 biology, the concept of viability is generally extended to a notion of having the capacity to  
356 divide in the future. Whether or not a cell divides in the future will be determined by the  
357 environment and the environment may change. Therefore it is difficult to assess viability with  
358 existing live/dead staining techniques, as these do not reveal the capacity for cell division  
359 after being stained. Indeed, some staining procedures can themselves be toxic (e.g., some  
360 DNA stains; Nebe von Caron, 2000) precluding a sort of cells on the basis of their staining  
361 characteristics and subsequent monitoring for cell division. Instead, live/dead staining  
362 methods test some physiological correlate of being alive, such as membrane permeability or  
363 enzyme activity. Such physiological correlates are ‘validated’ by abolishing them via cell  
364 killing with heat, chemical fixation or some other method. Since it is possible to generate a



365 complicated spectrum of states with such methods, making simple categorisation difficult,  
366 and the performance of the stains is variable between species (Brussaard et al. 2001), the use  
367 of live/dead stains has been limited in eukaryotic microbial ecology (Garvey et al. 2007).  
368 Nevertheless, these methods are at present the ‘state of the art’ and they have given valuable  
369 insight into the role of mortality in the microbial foodweb (Veldhuis et al. 2001). We show  
370 here that the coccolithophore *Emiliana huxleyi* has a very different response to growth  
371 limitation than the diatom *Thalassiosira pseudonana*. Benthic ‘resting stages’ are known in a  
372 number of *Thalassiosira* species (Lewis et al. 1999) but during the decline in our cultures we  
373 saw no obvious change in cell morphology. The ability to form resting stages has not been  
374 recorded in this strain/clonal isolate, and even if this ability did exist, it may have been lost in  
375 culture. *T. pseudonana* biomass remained constant for approximately 8 days before cell loss  
376 due to lysis became apparent (Fig. 1A) and throughout this period the efficiency of PS II  
377 declined in a pattern similar to that seen in *T. weissflogii* (Berges and Falkowski 1998) likely  
378 indicating a process of intracellular protein degradation brought about by nitrogen  
379 deprivation. Such internal degradation leads to a dismantling of the photosynthetic apparatus  
380 and the loss of photosynthetic pigment fluorescence. Both of these processes were very clear  
381 in our dataset; the loss of pigment fluorescence (‘chlorosis’; Geider et al. 1993) correlated  
382 with decreased enzyme activity and increased membrane permeability. This process was  
383 especially clear in the diatom but a more subtle process occurred in the coccolithophore.  
384 Fluorescence due to CaspACE binding did not increase during the decline in diatom biomass.  
385 Using the same strain of *T. pseudonana* (CCMP 1335) Bidle and Bender (2008) noted  
386 increased CaspACE binding (expressed as % of cells stained) during the cell lysis of *T.*  
387 *pseudonana* after stationary phase. Even higher binding was observed in Fe-limited biomass  
388 declines, and CaspACE binding was most prominent in cells with low fluorescence.  
389 Upregulation of caspases may therefore be more likely under Fe-limited conditions. An

390 ongoing difficulty in the use of caspase-activity stains in the interpretation of cell death  
391 processes is the lack of good positive controls. Cell differentiation to a resting stage is not a  
392 recognised pathway in coccolithophores, which may instead switch to a motile, haploid form  
393 during stressful conditions and thereby exploit a different ecological niche (Frada et al. 2008).  
394 However, the persistence of *E. huxleyi* during stationary phase in our study did not seem to be  
395 accompanied by meiosis, as assessed by periodic microscopy on our cultures. Increases in  
396 intracellular enzyme activity were clear from both CMFDA and CaspACE results,  
397 highlighting perhaps the requirement for hydrolytic enzymatic activity to be present in the cell  
398 for the successful detection of caspase-like activity. In the absence of other measurements  
399 (*see below*), there are three interpretations of increased CaspACE binding in *E. huxleyi*; 1) an  
400 increase in proteolytic activity within the cell related to a shift to a low metabolic state (which  
401 nevertheless retains photosynthetic pigmentation), or 2) intracellular reorganisation related to  
402 the induction of meiosis, or 3) programmed cell death (PCD) in moribund cells, potentially  
403 leading to an apoptotic morphology but with intact plasma membranes (the timing of  
404 membrane permeability failure may therefore be late in *E. huxleyi* PCD). Of these two  
405 possibilities we suggest that 1) or 2) is the safest interpretation because we do not have  
406 accompanying measurements of the other processes thought to be part of PCD and which  
407 would result in apoptosis (e.g., DNA fragmentation, phosphatidylserine inversion). Additional  
408 complications in the interpretation of the CaspACE data are that caspases may have  
409 alternative functions to PCD (Lamkanfi et al. 2007); in general, the clan to which caspases  
410 belong (clan CD, family C14) is poorly understood in protists (Vercammen et al. 2007).

411         Although our two species showed different responses to growth limitation in many  
412 respects, one common element was the formation of low-red or chlorotic cells. As a  
413 proportion of the total cell population chlorotic cells became more abundant in the diatom

414 cultures. The formation of chlorotic cells has been well noted before, in diatoms  
415 (*Phaeodactylum tricornutum*; Geider et al. 1993) and also in cyanobacteria (*Synechococcus*  
416 PCC 7942; Sauer et al. 2001). After the onset of nitrogen deprivation *Synechococcus* PCC  
417 7942 shows an immediate and substantial reduction in protein content leading to the  
418 formation of an ultra-low metabolism resting stage (Sauer et al. 2001). In *P. tricornutum* cell  
419 pigmentation changes rapidly as part of an adaptive and reversible response to self-shading  
420 thereby tuning photosynthetic activity to the available resources. Given our dataset it appears  
421 the response of *E. huxleyi* to nutrient limitation resembles that of *Synechococcus* in that whilst  
422 there was an immediate change in pigment content per cell, photosynthetic efficiency was  
423 unchanged and there was also no change in the pigment profile. Such a conclusion is  
424 reinforced by the recent finding that the high PSII repair capability of *E. huxleyi* means that it  
425 is well-adapted to endure nutrient deplete conditions (Loebl et al. 2010). In contrast, *T.*  
426 *pseudonana* showed a rapid decline in photosynthetic efficiency as pigment content declined  
427 and the pigment profile also changed. It is possible that the formation of chlorotic cells had  
428 different causes: in *E. huxleyi*, where the proportion of chlorotic cells did not increase as  
429 much as in the diatom population, the ultimate cause of cell chlorosis may have been cell  
430 cycle stage at a critical point in the onset of nutrient deprivation whereas in *T. pseudonana*,  
431 the higher proportion of chlorotic cells after nutrient deprivation suggests that all cells were  
432 destined to share the same fate. These two ideas are not mutually exclusive however since we  
433 did not assess the degree of cell-cycle synchrony; it may have been that the *T. pseudonana*  
434 cells were in synchronised division at the onset of nutrient deprivation. This seems unlikely;  
435 diatom cultures often require an experimental treatment (such as silica starvation) to induce  
436 synchrony (Hildebrand et al. 2007) and were therefore unlikely to be undergoing synchronous  
437 division. Resolving population cell cycle stage in parallel with assessments of physiological  
438 staining would be beneficial in further investigations of these responses. In conclusion,

439 CMFDA and SYTOX-green worked well as indicators of changing cell condition and yielded  
440 robust information. Our dataset highlights the necessity of making observations over a  
441 relatively long period in order to gather context and to avoid simple categorisations  
442 (live/dead) without such context. The increase in *E. huxleyi* CMFDA fluorescence during the  
443 stationary phase for example, clearly represents a process of cellular reorganisation, but cells  
444 did not become 'more alive'. Simplifications about cell states (e.g., 'active' and 'inactive')  
445 remain difficult using existing methods. Bacterioplankton, for example, display an enormous  
446 range of metabolic states in natural populations (Smith and del Giorgio 2003; Pirker et al.  
447 2005). Development of simultaneous and multi-staining approaches in eukaryotic  
448 microbiology should help in revealing all, or most, of the physiological heterogeneity within  
449 these populations.

450         This is the first study to investigate the formation of chlorophyll oxidation (allomer)  
451 products in conjunction with measurements of photosynthetic efficiency and loss of cell  
452 viability in phytoplankton cultures. The chlorophyll oxidation products detected,  
453 methoxychlorophyll and hydroxychlorophyll, are common products in laboratory studies of  
454 chlorophyll allomerisation reactions (Hynninen and Hyvärinen 2002; Jie et al. 2002).  
455 Methoxychlorophyll *a* however, has not been reported previously in eukaryotic  
456 phytoplankton. Methoxychlorophyll *a* and hydroxychlorophyll *a* increased relative to  
457 chlorophyll *a* from day 30 onwards in *T. pseudonana* cultures, by which point the dark-  
458 acclimated  $F_V:F_M$  had declined from 0.6 to 0.1. In contrast to *T. pseudonana*, the relative  
459 concentration of hydroxychlorophyll *a* and methoxychlorophyll *a* remained constant in *E.*  
460 *huxleyi*, as did the dark-acclimated  $F_V:F_M$  and percentage of SYTOX-green stained cells.  
461 Similarly, Bale (2010) found that the relative proportion of hydroxychlorophyll *a* remained  
462 constant in *E. huxleyi* over a 40 day period in batch culture. In *T. pseudonana*, the reduction in  
463 maximum PS II efficiency and increase in the relative abundance of chlorophyll oxidation

464 products preceded the increase in the percentage of cells labeled with SYTOX-green. The  
465 relative increase in chlorophyll alteration products may therefore serve as an early indicator of  
466 loss of cell viability. Although methoxychlorophylls have not been reported previously in  
467 pigment studies of senescent phytoplankton, detritus or sediments they have been detected in  
468 cyanobacteria (R.A. Airs unpubl. data) and further high resolution LCMS studies may reveal  
469 methoxychlorophyll to be a common early transformation product in phytoplankton.  
470 Hydroxychlorophyll *a* has been detected in field samples from phytoplankton blooms in the  
471 Celtic Sea and North Atlantic (Walker and Keely 2004; Bale 2010), and chlorophyll allomer-  
472 type components are commonly detected in field samples, even when routine rather than high  
473 resolution HPLC methods are applied (R.A. Airs unpubl. data). From the higher relative  
474 abundance of methoxychlorophyll *a* than hydroxychlorophyll *a* in our cultures, the detection  
475 of hydroxychlorophyll *a* in field samples indicates that the likelihood of detecting  
476 methoxychlorophyll *a* in field samples is good. The effect of these early chlorophyll  
477 alterations on the overall light absorption of the cell, and hence the potential of these  
478 alterations to be detected by remote methods is, however, unknown. A trace of pheophytin *a*  
479 (magnesium-free chlorophyll *a*) was detected in both cultures throughout the experiment (data  
480 not shown), contributing at levels <10% of the other chlorophyll alteration products detected.  
481 Pheophytin *a* has been shown to be present in healthy cells, due to its role as a primary  
482 electron acceptor of Photosystem II (Klimov 2003). Both chlorophyllide *a*, and its  
483 magnesium-free counterpart pheophorbide *a*, have been associated with senescence in earlier  
484 studies (Jeffrey and Hallegraeff 1987; Louda et al. 2002). These compounds were not  
485 detected, however, during this study. How senescence is defined within an experiment, the  
486 method of senescence induction, the timescale of experiments as well as the presence or  
487 absence of cellular enzymes (e.g., chlorophyllase) are likely to influence the specific  
488 alterations of chlorophyll *a*.

489           There are a number of sources and sinks of DMS and its precursor DMSP within the  
490 microbial foodweb. The intracellular concentration of DMSP in phytoplankton cells is the  
491 primary driver of ecosystem DMS emission, and certain microalgae synthesize DMSP in  
492 response to environmental factors such as light (Archer et al. 2010) and nitrogen depletion  
493 (Bucciarelli and Sunda 2003). DMSP can be released from algal cells by grazing and viral  
494 lysis and these pathways may also elevate DMS levels by bringing algal enzymes that release  
495 DMS from DMSP into more intimate contact with the substrate (Stefels et al. 2007). In  
496 addition bacteria demethylate DMSP, release DMS from DMSP and oxidise DMS to DMSO  
497 (Schaefer et al. 2010). Depending upon the bacterial genera present and pathways involved  
498 the DMS concentration can increase or decrease. However, it is interesting to note that the  
499 direct release by phytoplankton cells is suggested by modelling work to be the dominant  
500 factor in explaining natural DMS seasonality (Gabric et al. 2008).

501           In order to be useful as an antioxidant or an overflow compound the intracellular  
502 concentration of DMSP would need to vary actively in response to environmental stress. To  
503 estimate intracellular DMSP concentration it is necessary to have an accurate estimate of cell  
504 volume. In coccolithophores, this is complicated by the presence of the coccolith layer, the  
505 coccosphere, around the cell and in diatoms the intracellular vacuolar space provides a similar  
506 complication. During the stationary phase, coccolithophore calcification can continue after  
507 cell division stops (Lakeman et al. 2009) potentially leading to multi-layered coccospheres.  
508 Acidification can remove coccoliths prior to cell volume measurement but unfortunately we  
509 did not do this in the present study so our conclusion of a constant  $DMSP_{cell}$  concentration in  
510 stationary phase *Emiliana huxleyi* is based on an assumption of increasing cell volume.  
511 Stefels et al. (2007) point out that cells generally decrease in volume with nitrogen starvation.  
512 It is possible that in the present study the cell volume decreased whilst overall coccosphere  
513 volume increased, in which case intracellular DMSP concentration would also have increased.

514 We recommend measuring acidified and non-acidified samples for volume estimates in future  
515 studies. The realisation of how important this can be is currently spreading with some studies  
516 (Archer et al. 2010) acidifying to make accurate estimates of cell volume whereas older  
517 studies tended not to do this. We are not aware of any studies quantifying vacuolar changes in  
518 *Thalassiosira pseudonana* during nutrient limitation and taking our data at face value the 50-  
519 fold increase in intracellular DMSP concentration with nitrogen starvation confirms our  
520 original hypothesis. In nutrient-replete culture diatoms generally have lower concentrations of  
521 DMSP than representatives of other major phytoplankton groups (Stefels et al. 2007), so it has  
522 often been assumed that diatoms cannot be a major source of DMS in the marine  
523 environment. However, considering the data presented here and elsewhere (Sunda et al. 2002;  
524 Bucciarelli and Sunda 2003; Harada 2009), alongside estimates that diatom primary  
525 production accounts for ~40% of the global total (Falkowski et al. 1998), it is clear that the  
526 overall diatom contribution may be greater than previously assumed.

527 Our study indicates that two important phytoplankton species have fundamentally  
528 different responses to nutrient deprivation. These different responses reflect the ecology of  
529 their groups in nature, and our assessment of physiological state reveals that *E. huxleyi* is  
530 much better able to cope with nutrient deprivation than *T. pseudonana*, through a cellular  
531 reorganisation which may involve caspase-like activity and DMSP production. *T. pseudonana*  
532 shows a substantial increase in DMSP concentration in response to nitrogen limitation and  
533 dies and lyses rapidly. We show for the first time that methoxychlorophyll *a* appears in *T.*  
534 *pseudonana* before membrane permeability is lost and lysis begins. Methoxychlorophyll *a*  
535 could therefore be a useful indicator of diatom senescence.

536 **References**

- 537 Airs, R. L., and B. J. Keely. 2000. A novel approach for sensitivity enhancement in  
538 atmospheric pressure chemical ionization liquid chromatography/mass spectrometry.  
539 Rapid Commun. Mass Spectrom. **14**: 125-128.
- 540 Airs, R. L., J. E. Atkinson, and B. J. Keely. 2001. Development and application of a high  
541 resolution liquid chromatographic method for the analysis of complex pigment  
542 distributions. J. Chromatogr. A. **917**: 167-177.
- 543 Archer, S. D., M. Ragni, R. Webster, R. L. Airs, and R. J. Geider. 2010 Dimethyl  
544 sulfoniopropionate and dimethyl sulfide production in response to photoinhibition in  
545 *Emiliania huxleyi*. Limnol. Oceanogr. **55**: 1579-2589.
- 546 Agustí, S. 2004. Viability and niche segregation of *Prochlorococcus* and *Synechococcus* cells  
547 across the Central Atlantic Ocean. Aquat. Micob. Ecol. **36**: 53-59.
- 548 Bale, N. 2010. Type I and Type II chlorophyll-*a* transformation products associated with  
549 phytoplankton fate processes. Ph.D. thesis, University of Bristol.
- 550 Behrenfeld, M. J., and E. Boss. 2006. Beam attenuation and chlorophyll concentration as  
551 alternative optical indices of phytoplankton biomass. J. Mar. Res. **64**: 431-451.
- 552 Berges, J. A., and P. G. Falkowski. 1998. Physiological stress and cell death in marine  
553 phytoplankton: induction of proteases in response to nitrogen or light limitation.  
554 Limnol. Oceanogr. **43**: 129-135.
- 555 Bidle, K. D., and S. J. Bender. 2008. Iron starvation and culture age activate metacaspases and  
556 programmed cell death in the marine diatom *Thalassiosira pseudonana*. Euk. Cell **7**:  
557 223-236.
- 558 Bidle, K. D., and P. G. Falkowski. 2004. Cell death in planktonic, photosynthetic  
559 microorganisms. Nature Rev. Microbiol. **2**: 643-655.



560 Brussaard, C. P. D., D. Marie, R. Thyrhaug, and G. Bratbak. 2001. Flow cytometric analysis  
561 of phytoplankton viability following viral infection. *Aquat. Microb. Ecol.* **26**: 157-  
562 166.

563 Bucciarelli, E., and W. G. Sunda. 2003. Influence of CO<sub>2</sub>, nitrate, phosphate, and silicate  
564 limitation on intracellular dimethylsulfoniopropionate in batch cultures of the coastal  
565 diatom *Thalassiosira pseudonana*. *Limnol. Oceanogr.* **48**: 2256-2265.

566 Charlson, R. J., J. E. Lovelock, M. O. Andreae, and S. G. Warren. 1987. Oceanic  
567 Phytoplankton, Atmospheric Sulfur, Cloud Albedo and Climate. *Nature* **326**: 655-661.

568 Falkowski, P. G., R. T. Barber, and V. Smetacek. 1998. Biogeochemical controls and  
569 feedbacks on ocean primary production. *Science* **281**: 200-206.

570 Frada, M., I. Probert, M. J. Allen, W. H. Wilson, and C. De Vargas. 2008. The "Cheshire Cat"  
571 escape strategy of the coccolithophore *Emiliania huxleyi* in response to viral infection.  
572 *Proc. Natl. Acad. Sci. U. S. A.* **105**: 15944-15949.

573 Franklin, D. J., C. P. D. Brussaard, and J. A. Berges. 2006. What is the role and nature of  
574 programmed cell death in microalgal ecology? *Eur. J. Phycol.* **41**:1-41.

575 Gabric, A. J., P. A. Matrai, R. P. Kiene, R. Cropp, J. W. H. Dacey, G. R. DiTullio, R. G.  
576 Najjar, R. Simó, D. A. Toole, D. A. del Valle, and D. Slezak. 2008. Factors  
577 determining the vertical profile of dimethylsulfide in the Sargasso Sea during summer.  
578 *Deep-Sea Res. II* **55**: 1505-1518.

579 Garvey, M., B. Moriceau, and U. Passow. 2007. Applicability of the FDA assay to determine  
580 the viability of marine phytoplankton under different environmental conditions. *Mar.*  
581 *Ecol. Prog. Ser.* **352**: 17-26.

582 Geider, R. J., J. Laroche, R. M. Greene, and M. Olaizola. 1993. Response of the  
583 Photosynthetic Apparatus of *Phaeodactylum-Tricornutum* (Bacillariophyceae) to  
584 Nitrate, Phosphate, or Iron Starvation. *J. Phycol.* **29**: 755-766.

585 Harada, H., M. Vila-Costa, J. Cebrian, and R. P. Kiene. 2009. Effects of UV radiation and  
586 nitrate limitation on the production of biogenic sulfur compounds by marine  
587 phytoplankton. *Aquat. Bot.* **90**: 37-42.

588 Harrison, P. J., R. E. Waters, and F. J. R. Taylor. 1980. A broad-spectrum artificial seawater  
589 medium for coastal and open ocean phytoplankton. *J. Phycol.* **16**: 28-35.

590 Hildebrand, M., L. G. Frigeri, and A. K. Davis. 2007. Synchronized growth of *Thalassiosira*  
591 *pseudonana* (Bacillariophyceae) provides novel insights into cell-wall synthesis  
592 processes in relation to the cell cycle. *J. Phycol.* **43**: 730-740.

593 Hynninen, P. H., and K. Hyvarinen. 2002. Tracing the allomerization pathways of  
594 chlorophylls by O<sup>18</sup>-labelling and mass spectrometry. *J. Org. Chem.* **67**: 4055-4061.

595 Jeffrey, S. W., and G. M. Hallegraeff. 1987. Chlorophyllase distribution in ten classes of  
596 phytoplankton: a problem for chlorophyll analysis. *Mar. Ecol. Prog. Ser.* **35**: 293-304.

597 Jie, C., J. S. Walker, and B. J. Keely. 2002. Atmospheric pressure chemical ionisation normal  
598 phase liquid chromatography mass spectrometry and tandem mass spectrometry of  
599 chlorophyll *a* allomers. *Rapid Commun. Mass Spectrom.* **16**: 473-479.

600 Keller, M. D., W. K. Bellows, and R. R. L. Guillard. 1989. Dimethyl sulfide production in  
601 marine-phytoplankton. *Am. Chem. Soc. Symp. Ser.* **393**: 167-182.

602 Keller, M. D., and W. Korjeff-Bellows. 1996. Physiological aspects of the production of  
603 dimethylsulfoniopropionate (DMSP) by marine phytoplankton, p. 131-142. *In* R. P.  
604 Kiene, P. T. Visscher, M. D. Keller and G. O. Kirst [eds.], *Biological and*  
605 *environmental chemistry of DMSP and related sulfonium compounds*. Plenum Press.

606 Klimov, V. 2003. Discovery of phaeophytin function in the photosynthetic energy conversion  
607 as the primary electron acceptor of Photosystem II. *Photosynth. Res.* **76**: 247-253.

608 Kromkamp, J., and R. Forster. 2003. The use of fluorescence measurements in aquatic  
609 ecosystems: differences between multiple and single turnover measuring protocols and  
610 suggested terminology. *Eur. J. Phycol.* **38**: 103-112.

611 Lakeman, M. B., P. Von Dassow, and R. A. Cattolico. 2009. The strain concept in  
612 phytoplankton ecology. *Harmful Algae* **8**: 746-758.

613 Lamkanfi, M., N. Festjens, W. Declercq, T. Vanden Berghe, and P. Vandenabeele. 2007.  
614 Caspases in cell survival, proliferation and differentiation. *Cell Death Differ.* **14**: 44-  
615 55.

616 La Roche, J., R. J. Geider, L. M. Graziano, H. Murray, and K. Lewis. 1993. Induction of  
617 specific proteins in eukaryotic algae grown under iron-deficient, phosphorus-deficient,  
618 or nitrogen-deficient conditions. *J. Phycol.* **29**:767-77.

619 Lewis, J., A. S. D. Harris, K. J. Jones, and R. L. Edmonds. 1999. Long-term survival of  
620 marine planktonic diatoms and dinoflagellates in stored sediment samples. *J. Plank.*  
621 *Res.* **51**: 343-354.

622 Loebel, M., A. M. Cockshutt, D. A. Campbell, and Z. V. Finkel. 2010. Physiological basis for  
623 high resistance to photoinhibition under nitrogen depletion in *Emiliana huxleyi*  
624 *Limnol. Oceanogr.* **55**: 2150-2160.

625 Louda, J. W, L. Liu, and E. W. Baker. 2002. Senescence and death related alteration of  
626 chlorophyll and carotenoids in marine phytoplankton. *Organic Geochem.* **33**: 1635-  
627 1653.

628 Marie, D., N. Simon, and D. Vaultot. 2005. Phytoplankton cell counting by flow cytometry, p.  
629 253-269. *In* R. A. Anderson [ed.], *Algal culturing techniques*. Elsevier Press.

630 Nebe-von-Caron, G., P. J. Stephens, C. J. Hewitt, J. R. Powell, and R. A. Badley. 2000.  
631 Analysis of bacterial function by multi-colour fluorescence flow cytometry and single  
632 cell sorting. *J. Microbiol. Meth.* **42**: 97-114.

633 Peperzak, L., and C. P. D. Brussaard. 2011. Flow cytometric applicability of fluorescent  
634 vitality probes on phytoplankton. *J. Phycol.* **47**: 692-702.

635 Pirker, H., C. Pausz, K. E. Stoderegger, and G. J. Herndl. 2005. Simultaneous measurement of  
636 metabolic activity and membrane integrity in marine bacterioplankton determined by  
637 confocal laser-scanning microscopy. *Aquat. Microb. Ecol.* **39**: 225-233.

638 Rudiger, W. 2006. Biosynthesis of chlorophyll *a* and *b*: the last steps, p. 189-200. *In* B.  
639 Grimm, R. J. Porra. W. Rudiger and H. Scheer [eds.], *Chlorophylls and*  
640 *bacteriochlorophyll*, 25. Springer.

641 Sauer, J., U. Schreiber, R. Schmid, U. Volker, and K. Forchhammer. 2001. Nitrogen  
642 starvation-induced chlorosis in *Synechococcus* PCC 7942. Low-level photosynthesis  
643 as a mechanism of long-term survival. *Plant Physiol.* **126**: 233-243.

644 Schafer, H., N. Myronova, and R. Boden. 2010. Microbial degradation of dimethylsulphide  
645 and related C-1-sulphur compounds: organisms and pathways controlling fluxes of  
646 sulphur in the biosphere. *J. Exp. Bot.* **61**: 315-334.

647 Segovia, M., and J. A. Berges. 2009. Inhibition of caspase-like activities prevents the  
648 appearance of reactive oxygen species and dark-induced apoptosis in the unicellular  
649 chlorophyte *Dunaliella tertiolecta*. *J. Phycol.* **45**: 1116-1126.

650 Simó, R. 2001. Production of atmospheric sulfur by oceanic plankton: biogeochemical,  
651 ecological and evolutionary links. *Trends Ecol. Evol.* **16**: 287-294.

652 Smith, E. M., and P. A. del Giorgio. 2003. Low fractions of active bacteria in natural aquatic  
653 communities? *Aquat. Microb. Ecol.* **31**: 203-208.

- 654 Stefels, J. 2000. Physiological aspects of the production and conversion of DMSP in marine  
655 algae and higher plants. *J. Sea Res.* **43**: 183-197.
- 656 Stefels, J., M. Steinke, S. Turner, G. Malin, and S. Belviso. 2007. Environmental constraints  
657 on the production and removal of the climatically active gas dimethylsulphide (DMS)  
658 and implications for ecosystem modelling. *Biogeochemistry* **83**: 245-275.
- 659 Steinke, M., G. Malin, S. M. Turner, and P. Liss. 2000. Determinations of dimethylsulphonio-  
660 propionate (DMSP) lyase activity using headspace analysis of dimethylsulphide  
661 (DMS). *J. Sea Res.* **43**: 233-244.
- 662 Sunda, W., D. J. Kieber, R. P. Kiene, and S. Huntsman. 2002. An antioxidant function for  
663 DMSP and DMS in marine algae. *Nature* **418**: 317-320.
- 664 Szymczak-Zyla, M., G. Kowalewska, and J. W. Louda. 2008. The influence of  
665 microorganisms on chlorophyll *a* degradation in the marine environment. *Limnol.*  
666 *Oceangr.* **53**: 851-862.
- 667 Turner, S. M., G. Malin, L. E. Bagander, and C. Leck. 1990. Interlaboratory Calibration and  
668 Sample Analysis of Dimethyl Sulfide in Water. *Mar. Chem.* **29**: 47-62.
- 669 Veldhuis, M. J. W., T. L. Cucci, and M. E. Sieracki. 1997. Cellular DNA content of marine  
670 phytoplankton using two new fluorochromes: taxonomic and ecological implications.  
671 *J. Phycol.* **33**:527-541.
- 672 Veldhuis, M. J. W., G. W. Kraay, and K. R. Timmermans. 2001. Cell death in phytoplankton:  
673 correlation between changes in membrane permeability, photosynthetic activity,  
674 pigmentation and growth. *Eur. J. Phycol.* **36**:167-177.
- 675 Vercammen, D., W. Declercq, P. Vandenabeele, and F. Van Breusegem. 2007. Are  
676 metacaspases caspases? *J. Cell Biol.* **179**: 375-380.

677 Walker, J. S., A. H. Squier, D. H. Hodgson, and B. J. Keely. 2002. Origin and significance of  
678  $^{13}\text{C}$ -hydroxychlorophyll derivatives in sediments. *Organic Geochem.* **33**: 1667-1674.  
679 Walker, J. S., and B. J. Keely. 2004. Distribution and significance of chlorophyll derivatives  
680 and oxidation products during the spring phytoplankton bloom in the Celtic Sea April  
681 2002. *Organic Geochem.* **35**: 1289-1298.

Table 1. Assignment of chlorophyll and related alteration products in cultures of *Emiliania huxleyi* and *Thalassiosira pseudonana*.

Peak no.	Main UV-vis absorption bands (nm)	Full MS and MS <sup>2</sup> ions <sup>a,b</sup>	Assignment
I	430, 664	Full MS: [M+H] <sup>+</sup> 887 (100); MS <sup>2</sup> (887): 869 ([M+H] <sup>+</sup> -18; 2), 609 ([M+H] <sup>+</sup> -278; 100), 591 ([M+H] <sup>+</sup> -278-18; 50), 549 ([M+H] <sup>+</sup> -278-60; 15)	Hydroxychlorophyll <i>a</i>
II	432, 664	Full MS: [M+H] <sup>+</sup> 869 (100); MS <sup>2</sup> (869): 837 ([M+H] <sup>+</sup> -32; 5), 593 ([M+H] <sup>+</sup> -276; 100), 533 ([M+H] <sup>+</sup> -276-60; 80)	Chlorophyll <i>a</i> <sub>p276</sub>
III	432, 664	Full MS: [M+H] <sup>+</sup> 887 (100); MS <sup>2</sup> (887): 869 ([M+H] <sup>+</sup> -18; 5), 609 ([M+H] <sup>+</sup> -278; 100), 591 ([M+H] <sup>+</sup> -278-18; 50), 549 ([M+H] <sup>+</sup> -278-60; 10)	Hydroxychlorophyll <i>a</i> '
IV	422, 664	Full MS: [M+H] <sup>+</sup> 901 (60), 869 (100); MS <sup>2</sup> (901): 869 ([M+H] <sup>+</sup> -32; 25), 623 ([M+H] <sup>+</sup> -278; 10), 591 ([M+H] <sup>+</sup> -278-32; 100), 559 ([M+H] <sup>+</sup> -278-32-32; 15), 531 ([M+H] <sup>+</sup> -278-32-60; 40); MS <sup>2</sup> (869): 591 ([M+H] <sup>+</sup> -278; 100), 559 ([M+H] <sup>+</sup> -278-32; 15), 531 ([M+H] <sup>+</sup> -278-60; 30)	Methoxychlorophyll <i>a</i>
V	420, 662	Full MS: [M+H] <sup>+</sup> 901 (90), 869 (100); MS <sup>2</sup> (901): 869 ([M+H] <sup>+</sup> -32; 2), 623 ([M+H] <sup>+</sup> -278; 60), 591 ([M+H] <sup>+</sup> -278-32; 60), 559 ([M+H] <sup>+</sup> -278-32-32; 5), 531 ([M+H] <sup>+</sup> -278-32-60; 50); MS <sup>2</sup> (869): 591 ([M+H] <sup>+</sup> -278; 100), 559 ([M+H] <sup>+</sup> -278-32; 5), 531 ([M+H] <sup>+</sup> -278-60; 30)	Methoxychlorophyll <i>a</i> '
VI	432, 664	Full MS: [M+H] <sup>+</sup> 871 (100); MS <sup>2</sup> (871): 839 ([M+H] <sup>+</sup> -32; 5), 593 ([M+H] <sup>+</sup> -278; 100), 533 ([M+H] <sup>+</sup> -278-60; 75)	Chlorophyll <i>a</i>

<sup>a</sup>All chlorophyll derivatives appear as demetallated ions due to post column demetallation prior to sequential mass scanning (Airs and Keely 2000; *see* Methods).

<sup>b</sup>Full MS: relative abundance shown in parentheses. MS<sup>2</sup>: Precursor ion indicated in parentheses. MS<sup>2</sup> ions: relationship to [M+H]<sup>+</sup> and relative abundance indicated in parentheses.

## Figure legends

Figure 1. (A) Cell number and cell volume, (B) Efficiency of Photosystem II (dark-adapted  $F_V:F_M$ ), and (C) In vivo fluorescence in duplicate *Emiliana huxleyi* and *Thalassiosira pseudonana* batch cultures (mean and standard error) during cell division, the transition from cell division to stationary phase, and the death phase (*T. pseudonana* only).

Figure 2. Representative biparametric plots of red and green fluorescence in *Emiliana huxleyi* and *Thalassiosira pseudonana* batch cultures. The plots indicate the process of chlorosis (the reduction in cellular pigment fluorescence over time) in batch cultures. At day 0 both species show single populations with consistently high red (pigment) fluorescence; by day 23 two populations are apparent and are highlighted by the regions overlaid on the plot. Cells transitional between the two states are visible, indicating that the low red population arises via chlorosis of the high red population.

Figure 3. Membrane permeability (SYTOX-green staining) during nutrient depletion in *Emiliana huxleyi* and *Thalassiosira pseudonana*. (A) shows representative biparametric plots for both species at day 23. (B) shows the % of SYTOX-stained cells over time (mean and standard error). Note that 'stained cells' =  $Q1+Q2$ .  $Q1$ =stained debris and stained 'low-red' cells,  $Q2$ =stained 'normal' cells,  $Q3$ =unstained normal cells and  $Q4$ =unstained debris and unstained low-red cells.

Figure 4. Hydrolytic enzyme activity (CMFDA staining) during nutrient depletion in *Emiliana huxleyi* and *Thalassiosira pseudonana*. A) shows representative biparametric plots for both species at day 23: note the clear separation of the *E. huxleyi* population into a 'high' and 'low' CMF population as indicated by the superimposed regions on the plot. B) shows relative % of high and low CMF cells over the course of growth and stationary phase in *E. huxleyi*. Finally, C) shows normalised CMF fluorescence within the high *E. huxleyi*



population and all *T. pseudonana* cells (mean and standard error). n.b. CMF fluorescence was normalised to a fluorescence standard, flowset beads (*see text*), which were analysed simultaneously.

Figure 5. Changes in CaspACE binding in normal cells (*see text*) during nutrient depletion in *Emiliana huxleyi* and *Thalassiosira pseudonana* batch cultures (mean and standard error). n.b. CaspACE fluorescence was normalised to a fluorescence standard, flowset beads (*see text*), which were analysed simultaneously.

Figure 6. Partial HPLC chromatogram (660 nm) showing elution position (relative to chlorophyll *a*) of chlorophyll alteration products detected. For peak assignments *see* Table 1.

Figure 7. (A) Ratio of total methoxychlorophyll *a* to Chl *a* and total hydroxychlorophyll *a* + chl *a* p<sub>276</sub> to Chl *a* in *T. pseudonana* and *E. huxleyi* and (B) ratio of total carotenoid to Chl *a* in *T. pseudonana* and *E. huxleyi* (mean and standard error) in nutrient-limited batch cultures.

Figure 8. (A) DMSP<sub>total</sub> ( $\mu\text{mol L}^{-1}$ ), (B) DMSP<sub>cell</sub> ( $\text{mmol L}^{-1}$ ), and (C) DMS ( $\text{nmol L}^{-1}$ ) in duplicate *Emiliana huxleyi* (circles) and *Thalassiosira pseudonana* (triangles) batch cultures (mean and standard error) over the batch growth cycle.

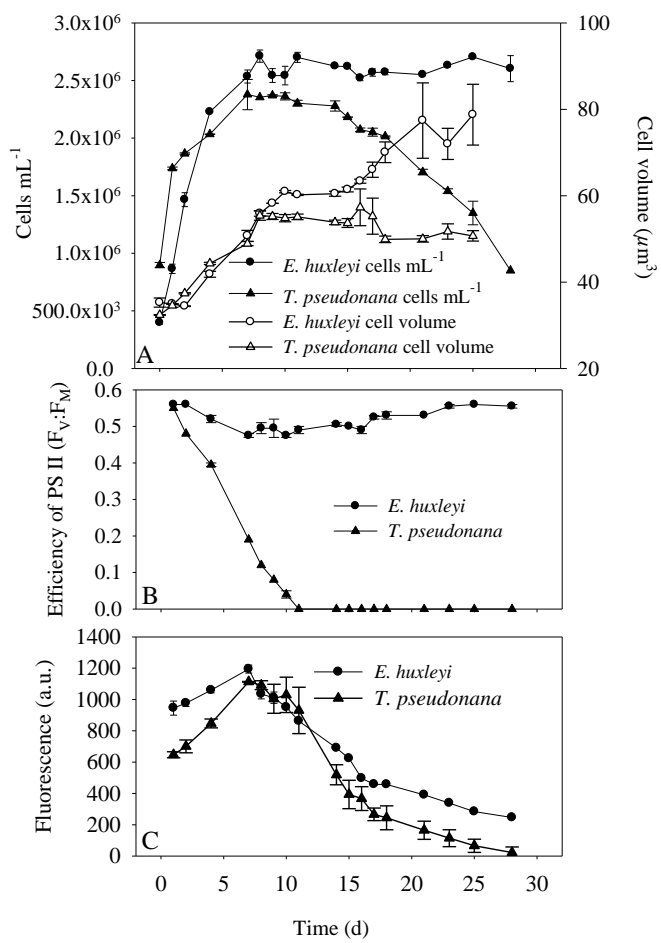


Figure 1

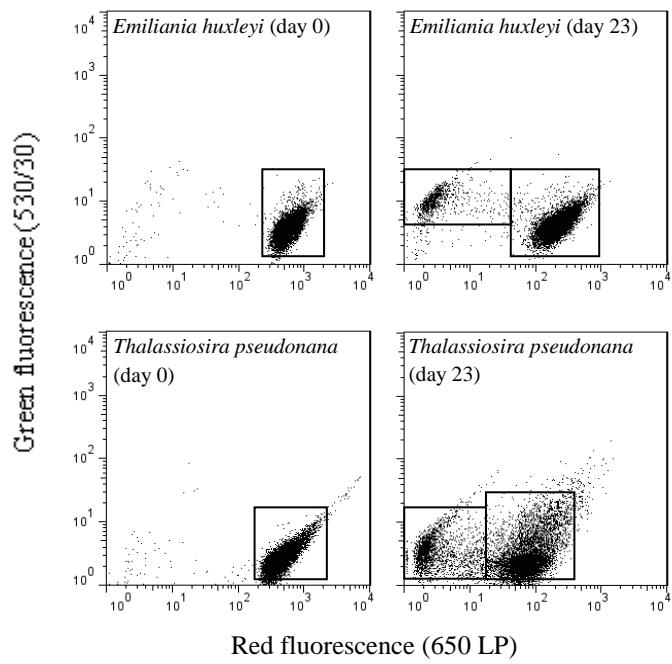


Figure 2

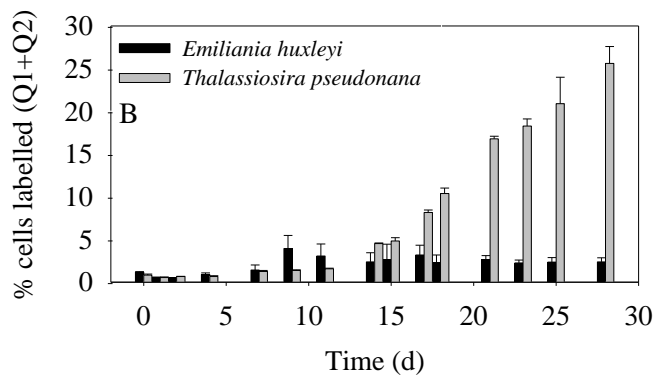
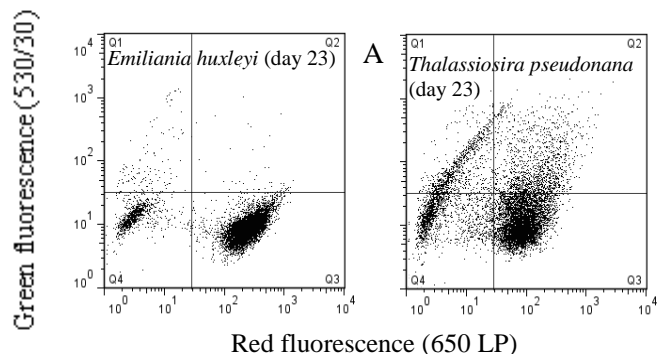


Figure 3

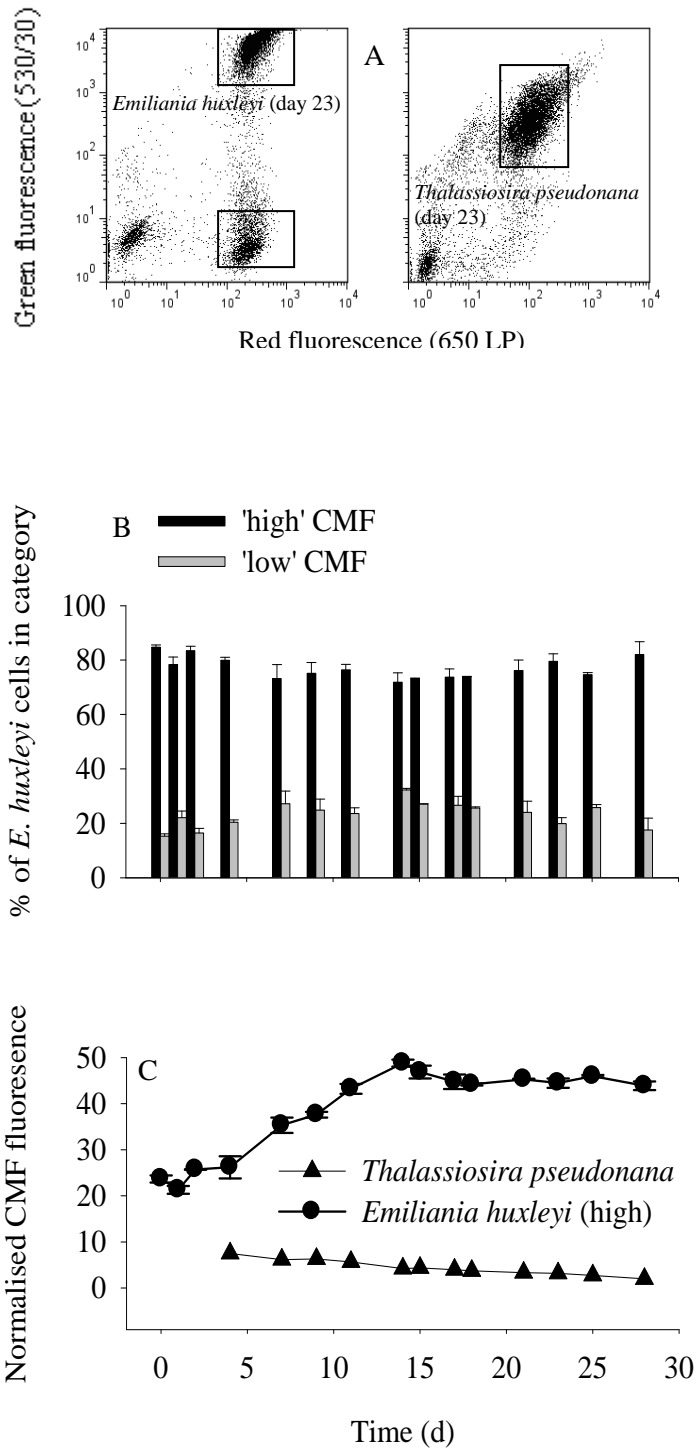


Figure 4

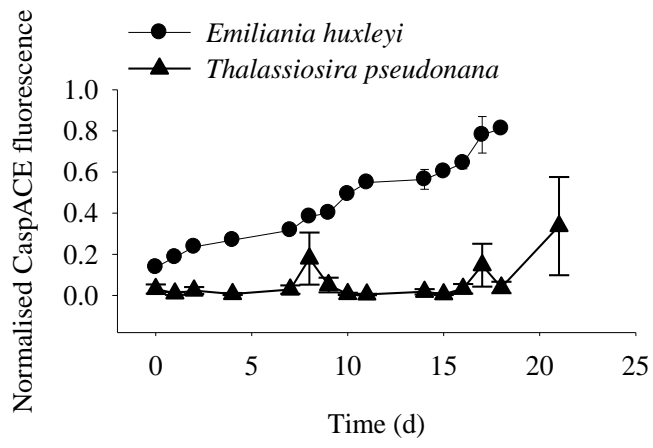


Figure 5

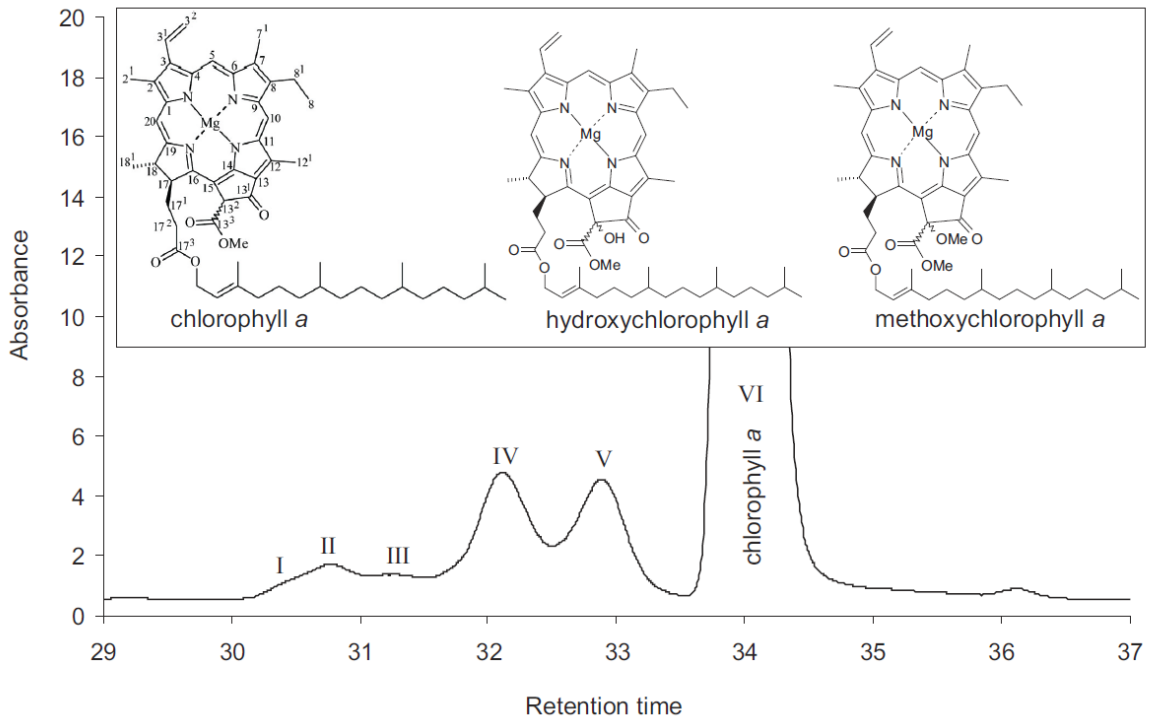


Figure 6

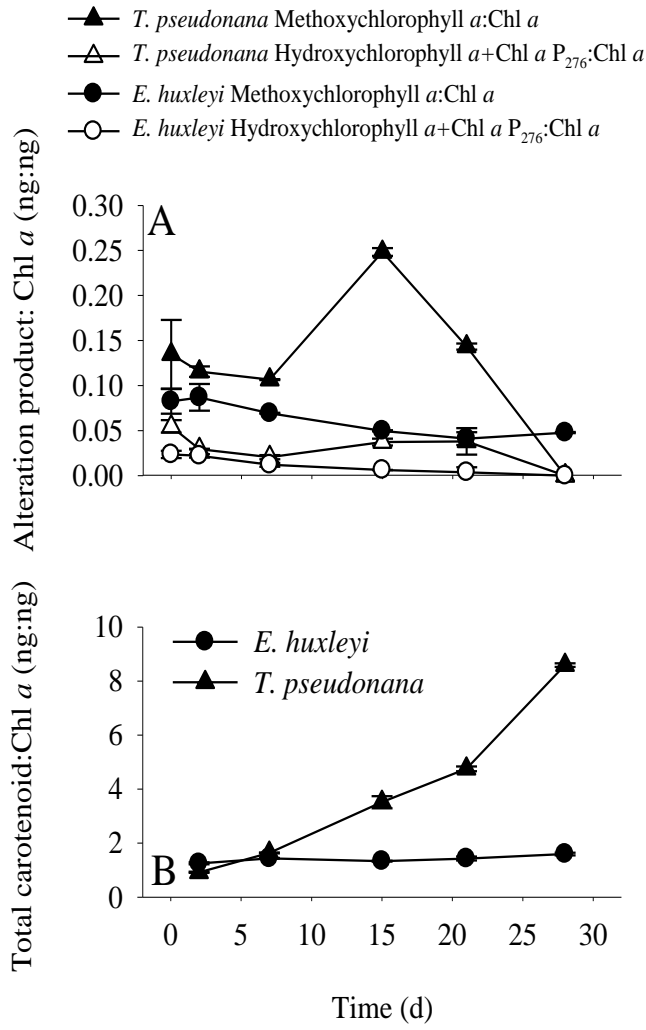


Figure 7



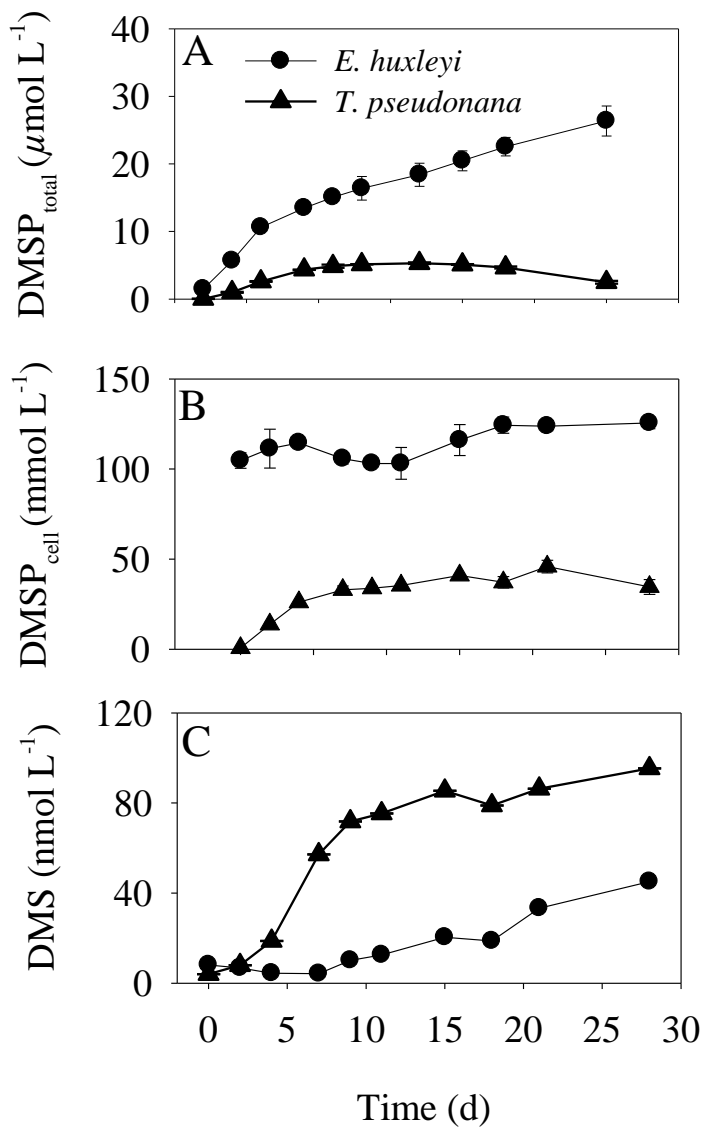


Figure 8